AOS Thesis

Intravitreal Administration of Stanniocalcin-1 Rescues Photoreceptor Degeneration with Reduced Oxidative Stress and Inflammation in a Porcine Model of Retinitis Pigmentosa

ROBERT H. ROSA JR., WANKUN XIE[1], MIN ZHAO[1], SHU-HUAI TSAI, GAVIN W. RODDY, MAXWELL G. SU, LUKE B. POTTS, TRAVIS W. HEIN, AND LIH KUO

• PURPOSE: To investigate the effect of stanniocalcin-1 (STC-1), a secreted polypeptide exhibiting multiple functions in cell survival and death, on photoreceptor degeneration in a porcine model of retinitis pigmentosa (RP).

• METHODS: P23H transgenic pigs (TG P23H) and wild-type hybrid littermates were obtained from the National Swine Resource and Research Center. Human recombinant STC-1 was injected intravitreally every 2 weeks from postnatal day 15 (P15) to P75. The contralateral eye was injected with balanced salt solution as a control. Electroretinography (ERG) and spectral domain optical coherence tomography (SD-OCT) were performed to evaluate retinal function and morphology in vivo at P90. Retinal tissue was collected for histologic analysis and molecular assays to evaluate the antioxidative and anti-inflammatory mechanisms by which STC-1 may rescue photoreceptor degeneration.

• RESULTS: Intravitreal injection of STC-1 improved retinal function in TG P23H pigs with increased photopic and flicker ERG a- and b-wave amplitudes. Greater integrity of the ellipsoid zone (EZ) band on SD-OCT and morphologic rescue with preservation of cone photoreceptors were observed in STC-1–treated TG P23H pigs. STC-1 altered gene expression in TG P23H pig retina on microarray analysis and increased photoreceptor specific gene expression by reverse transcription–polymerase chain reaction analysis. STC-1 significantly decreased oxidative stress and the expressions of NLRP3 inflammasome, cleaved caspase-1, and IL-1β in TG P23H pig retina.

• CONCLUSIONS: Intravitreal administration of STC-1 enhances cone photoreceptor function, improves EZ integrity, and reduces retinal degeneration through antioxidative and anti-inflammatory effects in a large animal (pig) model of the most common form of autosomal dominant RP in the United States. (NOTE: Publication of this article is sponsored by the American Ophthalmological Society. Am J Ophthalmol 2022;239: 230–243. © 2022 The Authors. Published by Elsevier Inc. This is an open access article under the CC BY license (http://creativecommons.org/licenses/by/4.0/))

Retinitis pigmentosa (RP) is a photoreceptor-degenerative disease that results from various mutations and is characterized by the death of rod photoreceptor cells, followed by the gradual demise of cone photoreceptors. Cone photoreceptor cell death causes central vision loss and eventual blindness in RP and advanced dry age-related macular degeneration (AMD). The prevalence of RP in the United States and Europe is about 1:3,500.[1] Mutations in the G protein–coupled receptor rhodopsin (RHO) gene in the rod photoreceptor are responsible for approximately 30% to 40% of autosomal dominant RP, and the proline-23-histidine (P23H) RHO gene mutation underlies the most common form of RP in North America, accounting for approximately 10% of all RP cases.[2] Although the molecular mechanisms that lead to rod and cone cell death are not yet fully understood, it is well documented that mutation-induced rod cell death is followed by mutation-independent cone cell death.[3-5] The degeneration of both rods and cones, in turn, triggers a remodeling of retinal circuitry and tertiary degeneration of inner retinal neurons.[5] Because of progressive, sequential loss of rod and cone photoreceptor cells, patients with RP typically present with night vision problems in adolescence, peripheral vision loss in young adulthood, and ultimately central vision loss in middle age.[6] Although many therapeutic approaches to prevent photoreceptor cell loss have been investigated, no effective, enduring treatments are currently available for the vast majority of

AJO.com Supplemental material at AJO.com
Accepted for publication March 12, 2022.

Department of Medical Physiology, Texas A&M University Health Science Center, Bryan, TX, USA (RR, WX, MZ, ST, LP, TH, LK); Department of Ophthalmology, Baylor Scott & White Eye Institute, Temple, TX, USA (RR, WX, MZ, MS, LP, TH, LK); Department of Ophthalmology, Mayo Clinic, Rochester, MN (GR)

Inquiries to Robert H. Rosa, Jr., Baylor Scott & White Eye Institute, Temple, Texas, USA.; e-mail: RRosa@TAMU.edu, Robert.Rosa@BSWHealth.org

[1] These two authors contributed equally to this work.

0002-9394/$36.00
https://doi.org/10.1016/j.ajo.2022.03.014

patients with inherited and acquired forms of retinal degeneration.[7] Mutations in more than 200 genes, including the RHO gene, have been identified in different forms of RP.[8] There is strong evidence to suggest a role for oxidative stress and neuroinflammation in the progression of retinal degenerative diseases.[9] Inflammatory processes and inflammatory cytokines might be involved in the development of RP in humans and animals.[10-12]

Stanniocalcin-1 (STC-1) is a secreted glycoprotein initially discovered in bony fish as a calcium-reducing factor for calcium-phosphate regulation in the fish gill.[13,14] STC-1 is also expressed in human tissues and organs, including the kidney, heart, liver, lung, prostate, adrenal gland, and ovary.[15-17] Mammalian stanniocalcins do not exhibit significant homology to other known proteins or contain previously recognized protein motifs.[18] STC-1 can promote angiogenesis in various experimental models,[19-23] suggesting its ability to facilitate cell/tissue survival. In contrast, additional studies have demonstrated inhibition of angiogenesis in other cells/tissues (eg, granulosa cells in the ovary), suggesting varying cell- or tissue-specific functions of STC-1.[24] Previous studies have suggested various roles for STC-1 in developmental and pathophysiological processes,[19,25,26] including cytoprotection via inhibition of programmed cell death, oxidative damage, and inflammation.[27-34] STC-1 was recently reported to inhibit proinflammatory cytokine production in vitro in activated microglia and to reduce neuroinflammation and oxidative stress in the hippocampus in a rat model of encephalopathy under systemic insults evoked by sepsis.[35] However, the action of STC-1 under local pathological stress remains to be characterized.

To date, the impact of STC-1 on ocular pathophysiology remains unclear. We recently showed that STC-1 protein is expressed in retinal pigment epithelial/choroidal tissue, with increased expression in areas treated with thermal laser photocoagulation.[36] In a rodent model of oxygen-induced retinopathy (OIR), Dalvin et al observed a modulatory effect by STC-1 with significantly worse OIR in STC-1 knockout mice.[37] Interestingly, Roddy et al recently reported that STC-1 lowers the intraocular pressure and is a downstream effector molecule in latanoprost signaling in rodent models of glaucoma.[38-40] We first discovered that intravitreal injection of adult mesenchymal stem/stromal cells (MSCs) can increase photoreceptor gene expression in the Royal College of Surgeons (RCS) rat,[41] presumably through upregulation of STC-1 expression in the MSCs.[27] Furthermore, intravitreal injection of human recombinant STC-1 rescued photoreceptors in the S334ter-3 rhodopsin transgenic and RCS rats due, in part, to reduced oxidative damage following upregulation of mitochondrial uncoupling protein-2.[41] In a follow-up study, intravitreal delivery of adeno-associated virus AAV-STC-1 caused long-term improvement in the structure and function of photoreceptors in 2 different RP models in rats.[42] These studies in different rodent models of RP support the potential therapeutic action of STC-1.

To further explore the in vivo retino-protective effect of STC-1 in a large animal model, we investigated the retinal function and morphology in pigs with Pro23His rhodopsin mutation (TG P23H),[43,44] a model of the most common form of human autosomal dominant RP in the United States. This pig model is characterized by a rapid-onset retinal degeneration with no significant rod function by electroretinography (ERG) at birth. We observed that intravitreal administration of STC-1 exerted multiple rescue effects on cone photoreceptor degeneration with improved retinal function, reduced photoreceptor cell death, decreased oxidative stress, modulated gene expression, and mitigated inflammation in TG P23H pigs. Based on these preclinical studies in a large animal model, we propose that STC-1 might be a promising therapeutic protein to enhance photoreceptor cell survival and homeostasis in retinal degenerative diseases. However, additional studies are needed to further investigate and elucidate the molecular mechanisms involved in the neuroprotective effect of STC-1.

METHODS

• **ANIMALS:** Male and female TG P23H and wild-type (WT) hybrid littermates were produced by inseminating domestic swine with semen from TG P23H mini swine (Founder line 53-1) as previously described[44] and were obtained from the National Swine Resource and Research Center at the University of Missouri in Columbia, MO. All pigs were kept under a 12-hour on/12-hour off light/dark schedule with free access to food and water. All procedures were performed with approval by the Institutional Animal Care and Use Committee at Baylor Scott & White Health and adhered to the Association for Research in Vision and Ophthalmology Statement for the Use of Animals in Ophthalmic and Vision Research.

• **INTRAVITREAL INJECTIONS OF STC-1:** Recombinant human STC-1 used in this study was purchased from BioVender Research and Diagnostic Products. According to the manufacturer's instructions, distilled water was added to a vial of STC-1 that was lyophilized in 20 mmol/L Tris buffer, 20 mmol/L NaCl to yield a final solution of 0.5 mg/ml. After sedation and induction with isoflurane anesthesia, the animal subject was prepared with topical povidone-iodine (Betadine) 5%. With sterile technique including the use of an eyelid speculum, an intravitreal injection of STC-1 protein (25 µL) in 50 µL of balanced salt solution (BSS) was performed (entry site 1 mm posterior to the limbus) in the right eye with a 30-gauge needle attached to a sterile syringe. The left eye was injected with vehicle (BSS) and served as an internal control. TobraDex ophthalmic ointment (Alcon) was applied immediately after the injection to reduce postinjection inflammation and the risk of infection. Recombinant human STC-1 (0.5 μg/μL,

50 μL) was injected intravitreally every 2 weeks from postnatal day 15 (P15) to P75.

• **ELECTRORETINOGRAPHY:** Full-field electroretinograms of the pigs were recorded at P90 with the ESPION System (Diagnosys LLC). After sedation and induction with isoflurane anesthesia, 2 contact ear electrodes were placed with conducting gel on the right and left ears. A contact lens electrode with lubricant gel was placed on the cornea of each eye. After 10 minutes of light adaptation, the photopic electroretinography (ERG) was recorded with a strobe flash intensity of 3.0 cd•s/m^2 and an interstimulus interval of 1 second. The 30-Hz flicker ERG (3.0 cd•s/m^2) was then recorded. An averaged response was constructed based on 5 to 10 presentations.

• **SPECTRAL DOMAIN OPTICAL COHERENCE TOMOGRAPHY:** The Heidelberg Spectralis HRA+OCT was used to document the microarchitecture of the retina in animal subjects as we previously described.[45,46] Both TG P23H and WT pigs were imaged at postnatal day 90 (P90). Before imaging, the animals were sedated, and all experimental protocols were performed under 2% to 4% isoflurane anesthesia. Pupils were dilated with 1% tropicamide eye drops (Bausch & Lomb Inc) before image acquisition. Artificial tears (Refresh Optive®, Allergan Inc) were administrated throughout the procedure to maintain corneal hydration. Images were obtained with the instrument set at a 30° field of view, using the Heidelberg Eye Explorer software (HEYEX version 6.6).

With the standardized fundus image, the position of the eye was maintained using the orientation of the optic disc, and all spectral domain optical coherence tomography (SD-OCT) scans were acquired in the same position. Seven vertical scans with an interscan distance at 240 μm were obtained along the vertical meridian through the optic disc by SD-OCT. To increase the signal-to-noise ratio, 100 frames were averaged per B-scan, and signal quality was greater than 25 db with the scan speed at 40,000 A-scans per second. The high-resolution mode was used with axial resolution at 3.9 μm digital and lateral resolution at 6 μm digital.

The reflective densities of the ellipsoid zone (EZ) bands were measured as previously described.[47-49] SD-OCT B-scans were exported and converted into 8-bit grayscale images. Images were then processed with the ImageJ software package (version 1.51j8; National Institutes of Health), and relative EZ intensities were measured as band intensity value divided by the external limiting membrane (ELM) intensity value along the vertical meridian from the optic disc and across the full length (7000 μm) of the SD-OCT scan in the superior retina.

The reflective density was calculated by averaging 6 measurements obtained at 500-μm intervals from 2500 μm to 5000 μm from the superior edge of optic disc in the superior retina in each eye. The overall average reflective density was calculated from 6 different eyes at P90.

The ONL thickness was calculated by averaging 6 measurements obtained at 500-μm intervals from 2500 μm to 5000 μm from the superior edge of optic disc in the superior retina in each eye. The overall percentage change in ONL thickness between P30 and P90 was calculated from 3 WT pigs and 5 TG P23H pigs.

• **TISSUE PREPARATION FOR MORPHOLOGICAL ANALYSES:** Pigs were euthanized via exsanguination under isoflurane anesthesia after SD-OCT image acquisition at P90. The eyes were enucleated and immediately placed in 4% paraformaldehyde (PFA). The anterior segment, lens, and vitreous were removed, leaving a posterior eyecup that contained the sclera, choroid, RPE, and neural retina. Every effort was made to avoid separation of the neuronal retina from the RPE during dissection and processing of the posterior eyecup. The posterior segment was then postfixed by immersion in 2% PFA/2% glutaraldehyde in phosphate-buffered saline at 4°C for 48 hours. Then, a 3-mm-wide strip of retinal tissue was dissected along the vertical meridian to include the optic disc and ora serrata. After rinsing, secondary fixation in buffered 1% osmium tetroxide, final rinsing, and dehydration, the tissue was embedded in Eponate 12 resin (Ted Pella). Blocks of retinal tissue were cut into 500-nm-thick sections using the RMC PowerTome X Ultramicrotome (Boeckeler Instruments), stained with 1% toluidine blue (Sigma-Aldrich), covered with a coverslip, and examined with light microscopy as previously described.[45,46]

• **MICROARRAY ASSAYS:** Microarray analysis was performed to evaluate the gene regulation as we previously reported.[41] Briefly, retinal tissue was collected on day 3 after a single injection of STC-1 (50 μg, 100 μL) at P30 in TG P23H pigs. A total of 250 ng of RNA from each sample was used for microarrays using GeneChip 3'IVT Express Kit (Affymetrix) according to the manufacturer's directions. Briefly, poly-A RNA controls were added into each sample to provide exogenous positive controls to monitor the eukaryotic target labeling process. T7 oligo(dT) primer was used to generate first-strand cDNA, followed by second-strand cDNA synthesis. To generate biotin-modified aRNA, in vitro transcription was performed, followed by purification and quantification of labeled aRNA. A total of 15 μg of aRNA was fragmented and hybridized (GeneChip Hybridization Oven 640; Affymetrix) onto pig arrays (GeneChip Porcine Genome Array #900624 or #900625, Affymetrix), followed by array washing and staining (GeneChip Fluidics Station 450; Affymetrix) with GeneChip Hybridization, Wash, and Stain Kit (Affymetrix). Arrays were scanned with GeneChip Scanner (Affymetrix), and images were checked for quality. Data were normalized using robust multi-array (RMA) algorithm, and gene level analysis was performed with Transcriptome Analysis Console Software (Thermo Fisher). To obtain up- and downregulated genes,

STC-1–treated samples were compared with BSS-treated samples, and expression level changes of at least 2-fold were considered significant.

• **REAL-TIME REVERSE TRANSCRIPTION–POLYMERASE CHAIN REACTION ASSAYS:** For RNA extraction, retinas were isolated by surgical excision at P90 after treatment with STC-1 0.5 μg/μL or BSS, 50 μL injection every 2 weeks starting at P15 (5 injections total). The isolated retina was immediately placed in RNA isolation reagent (RNA Bee, Tel-Test Inc) and frozen at −80°C. The samples were rapidly thawed and homogenized on ice, and total RNA was extracted (RNeasy Mini kit; Qiagen). cDNA was generated by reverse transcription (SuperScript III; Invitrogen) using 1 µg total RNA. Real-time amplification was performed using TaqMan Universal PCR Master Mix (Applied Biosystems). PCR probe sets and TaqMan Gene Expression Assay kits (Applied Biosystems) were used to measure gene expression (Phosducin: XM_003130382.3; Recoverin: XM_013981323.1; Cone transducing α-subunit (GNAT2): XM_021090070.1; MWL cone opsin: AY693774.1; SWL cone opsin: NM_214090.1; and 18s: NR_046261.1). Values were normalized to 18s RNA and expressed as a fold change compared to the BSS control eye.

• **ELISAS FOR MARKERS OF OXIDATIVE DAMAGE:** For protein extraction, retina was collected at P90 after treatment with a STC-1 0.5 μg/μL or BSS, 50 μL, injection every 2 weeks starting at P15 (5 injections total). The retinal tissue was then sonicated on ice in a Tris–ethylenediaminetetraacetic acid (EDTA) solution containing protease inhibitor cocktail (Roche). After centrifugation at 12,000 rpm at 4°C for 20 minutes, the supernatant was assayed for protein carbonyl content (OxiSelectTM Protein Carbonyl ELISA Kit, Cell Biolabs, Inc) or nitrotyrosine content (OxiSelectTM Nitrotyrosine ELISA Kit, Cell Biolabs, Inc) in accordance with the manufacturer's instructions.

• **WESTERN BLOT ANALYSIS:** The retina was isolated from eyecups at P90 after treatment with STC-1 0.5 μg/μL or BSS, 50 μL injection every 2 weeks starting at P15 (5 injections total) and then lysed with Tissue Extraction Reagents (Invitrogen) plus a supplement of protease inhibitor cocktail according to the manufacturer's instructions. Protein concentrations were determined with BCA assay kit (Pierce Biotechnology) in accordance with the manufacturer's instructions. Protein extracts (50 µg protein per sample) were subjected to 10% sodium dodecyl sulfate–polyacrylamide gel electrophoresis (SDS-PAGE) and then transferred to nitrocellulose membranes (Bio-Rad). The membranes were then incubated in 5% skim milk for 1 hour at room temperature, followed by overnight incubation in blocking buffer containing 1 of the following primary antibodies: NLRP3 (1:1000, Catalog #15101, Cell Signaling Technology), IL-1β (1:1000, Catalog #12703, Cell Signaling Technology), cleaved caspase-1 (c-caspase-1, 1:1000, Catalog #4199, Cell Signaling Technology), and β-actin (1:1000, Catalog #4970, Cell Signaling Technology) at 4°C. The next day, membranes were washed in 0.1% Tween in 1X PBS and incubated with horseradish peroxidase–conjugated secondary antibody for 1 hour at room temperature. Proteins of interest were detected with enhanced chemiluminescent reagents (Pierce Biotechnology). Membranes were stripped after incubation with primary antibodies for NLRP3, IL-1β, and c-caspase-1 and reprobed to detect β-actin on the same membrane. The ratios of NLRP-3, IL-1β, and c-caspase-1 expressions to β-actin expression were determined. These values from the treatment groups were normalized to the average of the normal control group and expressed as a relative ratio for comparison.

• **STATISTICAL ANALYSIS:** All data are presented as mean ± SEM and were analyzed using GraphPad Prism 9.3.0 (GraphPad Software). Two-way analysis of variance followed by the Tukey test was used in multiple group comparisons. Differences were considered significant at $P < .05$.

RESULTS

• **STC-1 IMPROVES NEURAL FUNCTION OF THE RETINA IN TG P23H PIGS:** To evaluate the effect of STC-1 on retinal function in P23H pigs, the ERG response was recorded in BSS- and STC-1–treated eyes in animals at P90. As shown in Figure 1A, no difference in the photopic ERG wave forms was observed between the BSS- and STC-1–treated eyes in the WT pigs. In contrast, the STC–1 treated eyes in the TG P23H pig demonstrated increased a- and b-wave amplitudes compared to the BSS-treated eyes (Figure 1B). The mean amplitude of the photopic a-wave and b-wave at a stimulus intensity of 3.0 cd•s/m^2 in STC-1–treated animal subjects were 90% and 59% greater, respectively, than the BSS-treated group of TG P23H pigs (Figures 1E, 1F). The 30-Hz flicker ERG was also measured to evaluate cone function. No significant difference in the 30-Hz flicker ERG wave forms was observed between BSS- and STC-1–treated eyes in WT pigs (Figure 1C). In contrast, increased 30 Hz ERG responses were observed in the STC-1–treated eyes in TG P23H pigs compared to the BSS-treated eyes in TG P23H pigs. The mean amplitudes of the 30-Hz flicker a- and b-waves in STC-1–treated eyes were 81% and 77% higher, respectively, than the BSS-treated eyes in the TG P23H pigs (Figure 1, G and H).

• **STC-1 INCREASES EZ BAND WIDTH, RELATIVE EZ INTENSITY, AND ONL THICKNESS IN TG P23H PIGS ON SD-OCT:** SD-OCT was used to assess the effect of STC-1 on the morphology of retinal layers in vivo. Figure 2A shows the

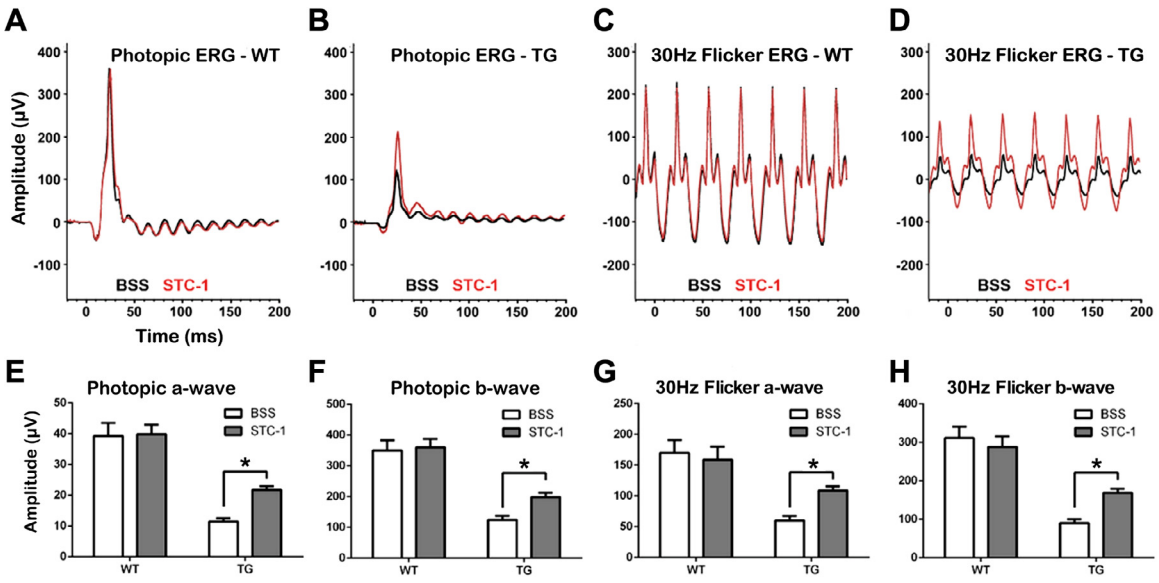

FIGURE 1. Stanniocalcin-1 (STC-1) improved photoreceptor function as measured by electroretinography (ERG) in P23H transgenic (TG) pigs. ERG analysis was performed at postnatal day 90 (P90) following intravitreal injection of STC-1 (0.5 μg/μL, 50 μL injection every 2 weeks starting at P15, 5 injections total) in wild-type (WT) and TG pigs. The photopic (A, B) and 30-Hz flicker ERG (C, D) were recorded at a light stimulus of 3.0 cd•s/m^2. The mean a- and b-wave amplitudes of the photopic (E, F) and 30-Hz flicker (G, H) ERG were decreased in TG pigs (n = 10). STC-1 significantly improved a- and b-waves, compared to treatment with balanced salt solution (BSS). STC-1 had no effect on the ERG in WT congenic pigs (n = 5). *$P < .05$, analysis of variance with Tukey test.

representative images of WT and TG P23H pigs treated with BSS or STC-1. No apparent adverse effect on retinal morphology was observed in STC-1—treated eyes on fundus imaging in WT animals. A vertical SD-OCT scan was performed to assess the width of the EZ band (Figure 2A, between yellow arrows) in the superior retina. No significant difference was observed in the width of the EZ band between BSS- and STC-1—treated eyes in WT pigs. However, an increased width of the EZ band was observed in STC-1—treated eyes compared to BSS-treated eyes in the TG P23H pigs. The mean width of the EZ band in the STC-1—treated eyes was 86% thicker than that in the BSS-treated eyes in TG P23H pigs (Figure 2B). In BSS treated TG P23H pig eyes, the ONL thickness in the superior retina decreased by approximately 60% between P30 and P90, whereas the ONL thickness after treatment with STC-1 decreased by approximately 40% in the superior retina (Figure 2C). No significant difference in ONL thickness in the superior retina was observed in the WT pig eyes treated with BSS or STC-1.

In addition to the differences in EZ band width, we assessed the relative intensity of the EZ band, a potential biomarker for the health of photoreceptors in retinal degenerative diseases. In WT pigs, no difference was observed in relative EZ intensity between the BSS and STC-1 groups. However, the relative EZ intensity was increased by 126% in STC-1—treated eyes compared to BSS-treated eyes in TG P23H pigs (Figure 3, A and B).

• **STC-1 RESCUED CONE PHOTORECEPTORS IN TG P23H PIGS:** To investigate the effect of STC-1 on retinal architecture, the histological analysis was performed at P90 after ERG and SD-OCT assessments. The ONL thickness was measured to evaluate photoreceptor survival. As shown in Figure 4A, no difference in ONL thickness was observed between BSS- and STC-1—treated eyes in the WT pigs. Histologic study of the retina revealed severe loss of the ONL (only one cell layer thick) in both BSS- and STC-1—treated TG P23H pigs. The number of cone photoreceptor cell nuclei was measured to assess the rescue effect of STC-1 on cone photoreceptor degeneration in the TG P23H pigs. Compared to BSS-treated eyes, the ONL cell count was increased by 70% in the STC-1 treatment group in TG P23H pigs (Figure 4B).

• **STC-1 ALTERED GENE EXPRESSION IN TG P23H PIG RETINA:** To assess early molecular changes with STC-1 treatment, total RNA was isolated from the retina of TG P23H pigs and evaluated using Affymetrix microarrays to identify differentially expressed genes. After STC-1 treatment in TG P23H pigs, 152 genes were upregulated >2-fold and 106 genes were downregulated >2-fold (Figure 5A). Three days after intravitreal administration of STC-1, upregulation of genes involved in signaling pathways for hypoxia response, integrins, TGFβ receptor, modulation of angiogenesis, regulation of apoptosis, NF-κB, protein kinase B, Wnt, and an

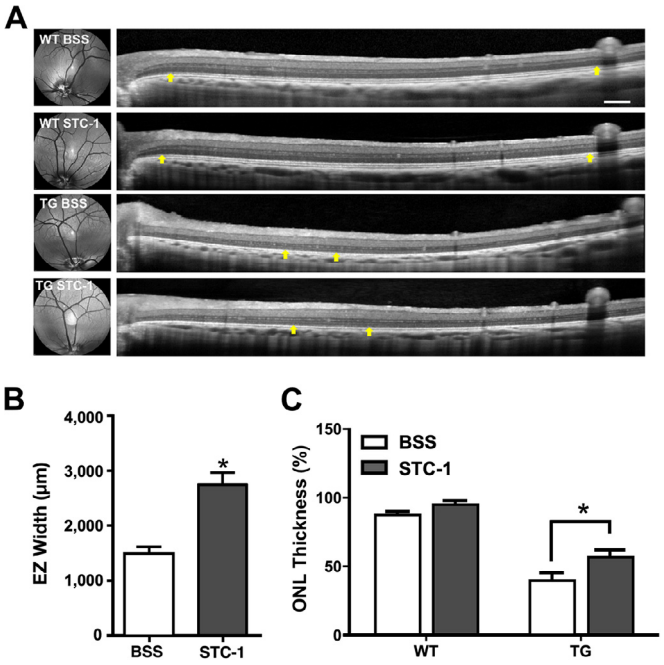

FIGURE 2. Stanniocalcin-1 (STC-1) increased ellipsoid zone (EZ) band width in the transgenic (TG) pig measured by spectral domain optical coherence tomography (SD-OCT). Fundus images and SD-OCT images were acquired in wild-type (WT) and TG pigs at P90. No apparent adverse effects on retinal morphology were observed in STC-1–treated eyes using multimodal retinal imaging. The EZ band (arrows) was observed along the whole scan area in WT pigs. In balanced salt solution (BSS)–treated control TG pigs, the EZ band was observed as an intermittent hyperreflective band (arrows) in a restricted area along the vertical meridian of the superior retina (A). A significant increase in the width of the EZ band was observed in STC-1–treated TG pigs (B). Between P30 and P90, outer nuclear layer (ONL) thickness in the superior retina decreased by approximately 60% and 40% in TG P23H pig eyes treated with BSS and STC-1, respectively (C). No significant difference in ONL thickness in the superior retina was observed in the WT pig eyes treated with BSS or STC-1. *$P < .05$. Scale bar = 200 μm.

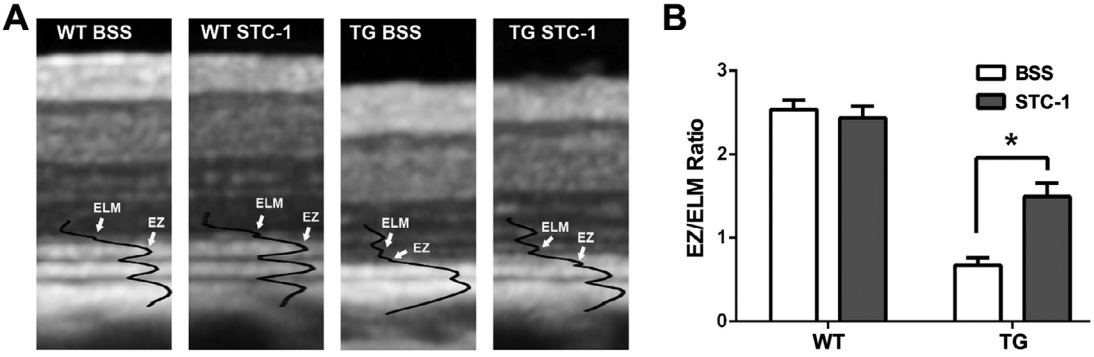

FIGURE 3. Stanniocalcin-1 (STC-1) increased relative ellipsoid zone (EZ) intensity in the transgenic (TG) pig. Spectral domain optical coherence tomography (SD-OCT) imaging was performed at P90 following injections of STC-1 in wild-type (WT) and TG pigs. Representative SD-OCT scans are shown, with the intensity profile of the outer retina acquired approximately 3000 μm from the optic nerve head in the superior retina (A). Note the increased thickness of the EZ compared to the external limiting membrane (ELM) in the SD-OCT images in both the WT and TG pig retina (A). The relative EZ intensity was measured as band intensity value divided by the ELM intensity value along the vertical meridian from the optic disc and across the full length (7000 μm) of the SD-OCT scan in the superior retina. Compared to WT pigs, the relative intensity of the EZ band was significantly decreased in TG pigs. The relative intensity of the EZ band was significantly increased in STC-1–treated TG pigs (B). *$P < .05$, analysis of variance followed by Tukey test.

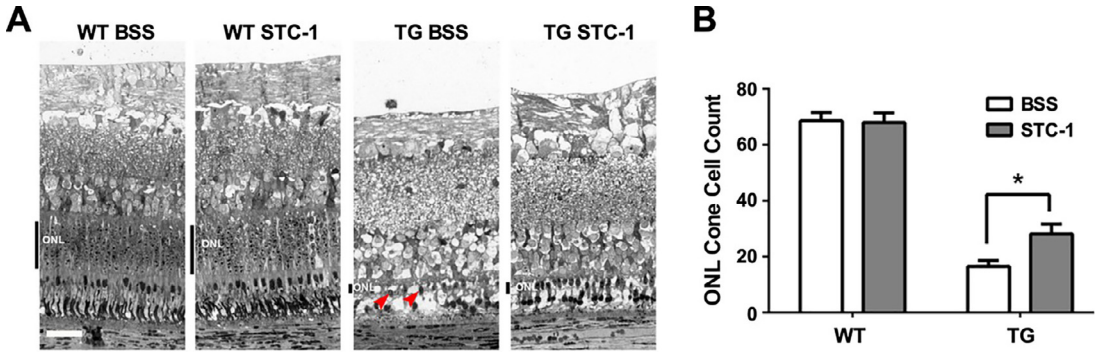

FIGURE 4. Stanniocalcin-1 (STC-1) injection rescued cones in P23H TG pigs. Note the pyknotic nuclei representing apoptotic photoreceptors (red arrows) in the outer nuclear layer (ONL, black vertical bar at left edge of photomicrographs) of the balanced salt solution (BSS)– treated TG pig (A). More cone nuclei and inner segments were present in the ONL of the superior retina at P90 after STC-1. The average number of cone cells in the ONL per 200-μm length of superior retina (600-μm segments, 3 sections per eye) was greater in STC-1–treated eyes (B). n = 6, *$P < .05$, analysis of variance with Tukey test. White scale bar = 20 μm.

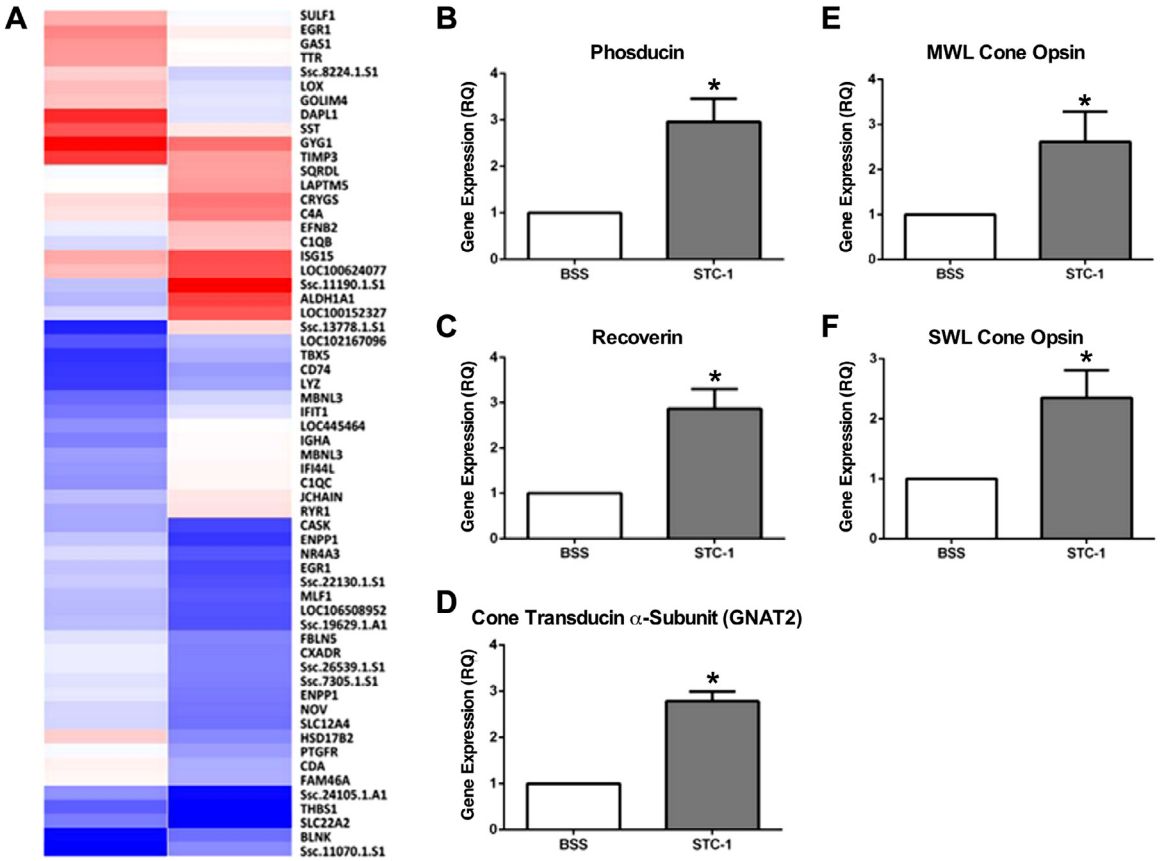

FIGURE 5. Stanniocalcin-1 (STC-1) altered photoreceptor gene expression. (A) Heat maps of genes upregulated or downregulated >2.5-fold by STC-1 treatment (right panel) compared to balanced salt solution (BSS) control (left panel). Retina was obtained for microarray on the third day after a single injection of STC-1 at P30. Microarray analysis revealed that 152 genes were upregulated (red) >2-fold and 106 were downregulated (blue) >2-fold in STC-1–treated eyes. (B) The mRNA expression for the photoreceptor-specific genes phosducin, recoverin, GNAT-2 (cone transducin α-subunit), MWL (green-sensitive) cone opsin, and SWL (UV-sensitive) cone opsin were upregulated in STC-1–treated retina collected at P90 (STC-1 0.5 μg/μL, 50 μL injection every 2 weeks starting at P15, 5 injections total). The mRNA levels of genes were normalized against 18s rRNA levels. n = 3. *$P < .05$, Student *t* test.

inflammatory/immune response (ADSL, ALDH1A2, ATP6V1C2, BAG6, CCL8, CD40, CDC6, DAB2, HPSE, IRF8, IGTA8, ITGB2, LRRN1, PLAU, RERG, RIPK3, TYK2, VAV1) was observed (Supplemental Table 1). At the same timepoint, downregulation of genes involved in intracellular receptor signaling, apoptosis, TGFβ receptor signaling, MAPK cascade, protein kinase B, PI3K pathway, protein kinase C signaling, ERK1/ERK2 cascade, NF-κB signaling, inflammatory response, angiotensin-activated signaling, oxidation-reduction process, cell redox homeostasis, protein folding, endoplasmic reticulum unfolded protein response, glial cell migration, angiogenesis, Wnt signaling, ER to Golgi vesicle–mediated transport, chemotaxis, semaphorin–plexin signaling, neurogenesis, and cilium assembly (ACSL4, AGTR2, ARL6IP5, CACNA2D2, DNAJB9, ERGIC1, ERO1A, GPD2, HTR2B, KIF3A, LOC100294704/LOC106510366, LOC100739844/LOC106507218, LOX, LRP6, MAP3K1, MSTN, NR4A3, PDIA3, PRKRA, SDHAF2, THY1, VCAN) was observed (Supplemental Table 2).

To examine gene expression changes related to photoreceptor survival at P90 after STC-1 treatment (0.5 μg/μL, 50 μL injection every 2 weeks starting at P15, 5 injections total), the photoreceptor-specific genes phosducin, recoverin, cone transducin α-subunit (GNAT2), MWL cone opsin, and SWL cone opsin were selected for analysis with quantitative polymerase chain reaction (qPCR). The expression levels of phosducin, recoverin, cone transducin α-subunit (GNAT2), MWL cone opsin, and SWL cone opsin were upregulated by 196%, 186%, 172%, 162% and 135% in STC-1–treated eyes compared to BSS-treated control group eyes (Figure 5B).

• **STC-1 DECREASED OXIDATIVE STRESS MARKERS IN TG P23H PIG RETINA:** Because oxidative stress and the inflammatory process are closely linked in retinal degeneration, the effects of STC-1 on oxidative stress and inflammatory markers were examined. As a product of ROS, protein carbonyl and 3-nitrotyrosine expressions were used as the index for oxidative damage in retinal degeneration. As shown in Figure 6, A and B, compared to BSS-treated TG P23H pig retina, the level of carbonyl and 3-nitrotyrosine decreased by 34% and 46%, respectively, in the STC-1–treated group.

• **STC-1 DECREASED NLRP3 EXPRESSION IN TG P23H PIG RETINA:** To determine the effect of STC-1 on retinal degeneration in relation to suppression of inflammation, the expression levels of NLRP3, c-caspase-1, and IL-1β were evaluated. Western blot analysis revealed increased expression of NLRP3, c-caspase-1, and IL-1β in TG P23H pig retina compared to WT pigs. The expression levels of NLRP3, c-caspase-1, and IL-1β were significantly decreased in eyes treated with STC-1 compared to the eyes treated with BSS in TG P23H pigs.

DISCUSSION

In this study using a large animal model of inherited retinal degeneration resembling human RP, intravitreal administration of STC-1 improved retinal function as measured by cone ERG responses, reduced photoreceptor degeneration as measured in vivo by EZ band width and relative EZ intensity with SD-OCT, and decreased bystander cone photoreceptor cell loss as measured by histologic analysis. The rescue effect by STC-1 appears to be multifactorial through the modulation of multiple signaling pathways, including apoptosis, inflammation, and oxidative stress. Thus, STC-1 could potentially act as a therapeutic protein and homeostatic agent to reduce photoreceptor cell loss (particularly cones) and to preserve central visual function in inherited, and possibly acquired, retinal degenerations.

Although multiple experimental models of retinal degeneration have been generated in rodents with a rod-dominated retina,[50-52] the lack of a cone-rich area of retina specialization is a major limitation in these models for studying the pathophysiology of and treatment strategies for cone photoreceptor degeneration in the early and later stages of RP. A specialized fovea or macula is not present in the pig retina; however, an area of high-density cones is present superior and temporal to the optic nerve head in the horizontal axis and simulates the macula in humans.[53] The porcine retina is characterized by a rod-to-cone ratio of approximately 8:1 compared to the human retina with a rod-to-cone ratio of 20:1.[53,54] Moreover, the size, anatomy (including the dual vascular supply to the retina), histology, vascular function, photoreceptor distribution, and immunology of the porcine eye are very comparable to those of the human eye.[55-61] Herein, a large animal model, the P23H rhodopsin transgenic pig (TG P23H, founder line 53-1) was used in the present study to address cone photoreceptor degeneration in a human-resembling model of the most common form of autosomal dominant RP in the United States. We recently addressed a gap in knowledge on the correlation between SD-OCT and histology, including electron microscopy, in the porcine retina, highlighting similarities with the human SD-OCT retinal imaging.[45,46] These previous studies provided us with normative/correlative SD-OCT and histologic data for the porcine retina and a foundation for future studies using the porcine model for retinal research. In another study, we found that retinal degeneration can be quantified longitudinally by measuring the width and relative intensity of the ellipsoid zone (EZ) band using SD-OCT in TG P23H pigs.[47] The SD-OCT measurements of the EZ corresponded to the histologic and ERG assessments of retinal degeneration in a time-dependent manner. In the current study, we used ERG and SD-OCT for in vivo study assessments of retinal function and morphology in the TG P23H transgenic pigs and the WT congenic control pigs. During the progression of

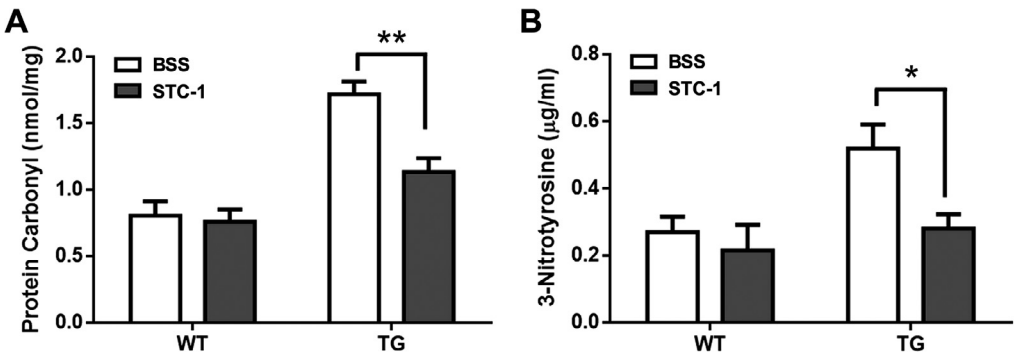

FIGURE 6. Intravitreal injection of stanniocalcin-1 (STC-10 decreased levels of 2 reactive oxygen species products in TG pig retina. The protein contents of carbonyl (A) and 3-nitrotyrosine (B) in transgenic (TG, n = 5) vs wildtype (WT, n = 3) pigs at P90 after STC-1 treatment (50 μL, 0.5 μg/μL) every 2 weeks between P15 and P90 are shown. The contralateral eye was injected with BSS (50 μL) as a control. *P < .05, **P < .01, analysis of variance followed by Tukey test.

retinal degeneration, scotopic retinal function never develops in TG P23H pigs, while cone photopic function develops up to P30 and declines rapidly at P60, with only one layer of cone nuclei remaining histologically at P90.[44,62] The rapidly progressive rod degeneration, coupled with the slower cone degeneration, makes this porcine RP model an excellent large animal model to study secondary or bystander cone degeneration.

Based on the rapidly progressive retinal degeneration in the TG P23H model as described above, we chose to use the photopic ERG to evaluate cone function and photoreceptor rescue after STC-1 treatment. The photopic and 30-Hz flicker ERG amplitudes were significantly increased after intravitreal injections of STC-1 in the TG P23H pig compared to BSS-injected control eyes (Figure 1). No apparent differences in ERG amplitudes were observed in the WT congenic controls treated with BSS or STC-1 (Figure 1). In this model of rapid photoreceptor degeneration, the measurement of ONL thickness with SD-OCT and histology may not provide an adequate assessment of photoreceptor survival or rescue after treatment with STC-1. However, we did observe greater preservation of ONL thickness in the superior retina in TG P23H eyes treated with STC-1 compared to BSS (Figure 2). Moreover, EZ integrity measured with SD-OCT can serve as a marker to evaluate the progression of retinal degeneration as previously described.[63] Assessments of EZ integrity include measurements of the EZ band width or thickness and the relative EZ intensity (EZ band intensity value divided by the external limiting membrane intensity value). The EZ band width (Figure 2) and relative EZ intensity (Figure 3) were significantly increased in the TG P23H pig eyes treated with STC-1. No significant differences were observed in EZ band width or relative EZ intensity in BSS- and STC-1—treated eyes in the WT congenic control animals (Figures 2 and 3). In addition to EZ integrity in rapid degeneration models, ONL cell counts can be used to assess histologic rescue of photoreceptor cells after therapeutic interventions. A significantly increased number of cone nuclei and cone inner segments was observed in eyes treated with STC-1 compared to those treated with BSS in the TG P23H pig (Figure 4). No significant differences in histologic appearance or ONL cells counts were noted in WT congenic control eyes treated with BSS or STC-1 (Figure 4), indicating the selective and specific effect of STC-1 on cell survival during the progression of RP.

In our previous studies in rodent RP models, we observed upregulation of genes associated with signaling pathways that promote neuroprotection and inhibit apoptosis and oxidative injury.[41,42] In the current study, microarray analysis of RNA isolated from TG P23H pig retina 3 days after intravitreal injection of STC-1 revealed modulation of signaling pathways involved in apoptosis, inflammatory response, angiogenesis, oxidation-reduction process, ER unfolded protein response, glial cell migration, and various protein kinase cascades (Figure 5A and Supplemental Tables 1 and 2). Interestingly, STC-1 triggered both upregulation and downregulation of genes involved in different signaling pathways, which affect specific biologic processes (eg, inflammation, apoptosis, and cell redox homeostasis). Moreover, STC-1 affected up- and downregulation of genes associated with the Wnt signaling pathways that employ nearby cell—cell or same-cell communication.[64,65] This is consistent with the reported physiological and pathophysiological role of STC-1 via autocrine/paracrine mechanism(s) in mammals.[66] Taken together, the results of our microarray analyses suggest that STC-1 is a functional protein that exerts multifaceted effects on gene expression in the retina through paracrine/autocrine signaling after intravitreal administration. Future studies will use rodent models with knockouts of specific molecular pathways to provide mechanistic data regarding the beneficial effects of STC-1 in the setting of retinal degeneration.

In addition to the early molecular changes in the retina observed by microarray analysis, intravitreal administration of STC-1 (every 2 weeks between P15 and P75, 5 in-

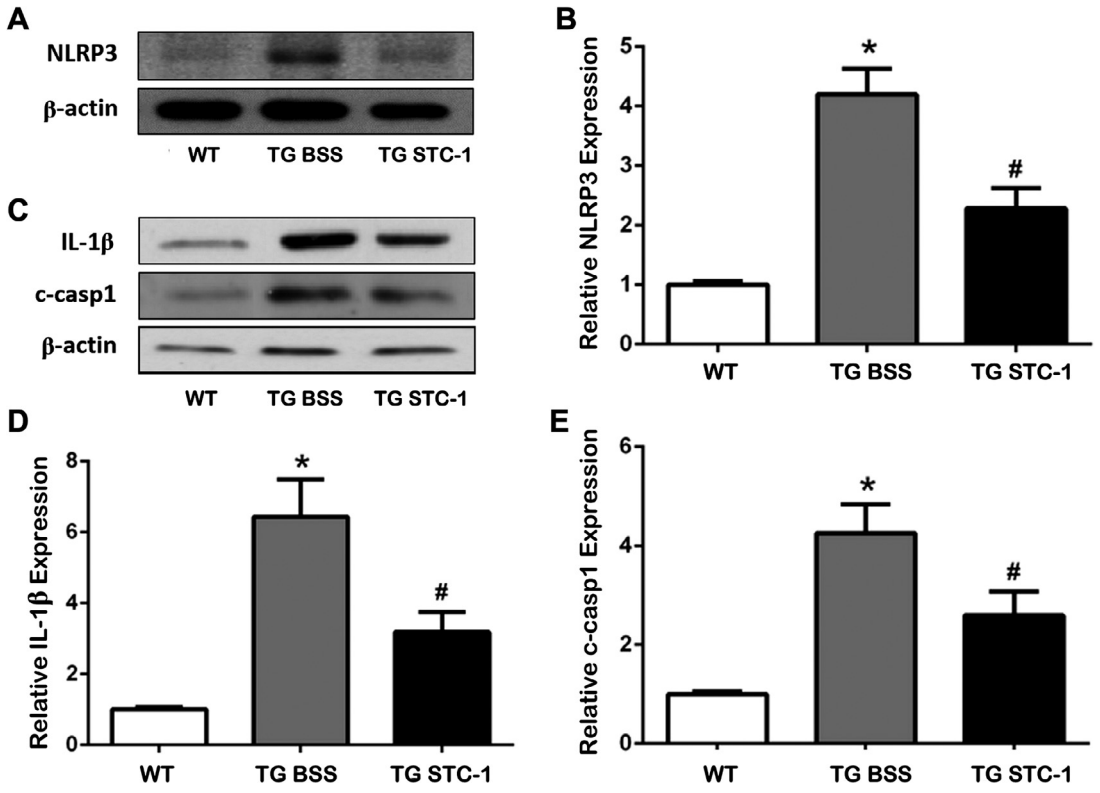

FIGURE 7. Intravitreal stanniocalcin-1 (STC-1) decreased NLRP3 expression in the retina of P23H TG pigs. A. NLRP3 protein expression was detected in the retina tissue of wild-type (WT; n = 5) and transgenic (TG; n = 5) pigs treated with balanced salt solution (BSS) or STC-1. B. NLRP3 protein expression was reduced in TG pig retina treated with STC-1. C. Expression levels of interleukin (IL)−1β and c-caspase-1 (c-casp1) were detected in the retina tissue of WT and TG pigs treated with BSS or STC-1. The expression levels of interleukin (IL)−1β (D) and c-caspase-1 (E) were reduced in TG pig retina injected with STC-1. *P < .05 vs WT, #P < .05 vs TG-BSS, 1-way analysis of variance followed by Tukey test.

jections total) increased the expression of photoreceptor-specific genes including phosducin, recoverin, cone transducin α-subunit (GNAT2), MWL cone opsin, and SWL cone opsin at P90 (Figure 5B). The upregulation of these photoreceptor-specific genes in STC-1−treated TG P23H pig retina is consistent with the observed histologic (cone photoreceptor cell) and functional (cone ERG) improvement by STC-1 in the diseased retina, particularly on cone photoreceptor survival.

To elucidate potential mechanistic pathways whereby STC-1 elicits the observed cone photoreceptor rescue in the TG P23H pig retina, we examined markers of oxidative injury/stress. Oxidative damage has been implicated in the demise of photoreceptors during the progression of RP.[5,67] We previously reported a reduction in 2 biomarkers of oxidative damage, carbonyl and nitrotyrosine proteins, in the retina of rat models of inherited retinal degeneration after intravitreal administration of STC-1.[41] In the TG P23H pig, we observed a similar decrease in the levels of these 2 protein adducts after intravitreal STC-1 treatment. The reduction in reactive oxygen species (ROS) generation might be, in part, a result of upregulation of mitochondrial uncoupling protein-2 by STC-1.[41,42,68] Interestingly, previous studies using immunogold electron microscopy and subcellular fractionation have revealed that cellular STC-1 immunoreactivity is confined mostly to the inner mitochondrial matrix, although the precise localization and nature of the receptors are largely unknown.[69] Recently, STC-1 was shown to operate as an "eat me" signal blocker through intracellular sequestration of calreticulin in mitochondria, thus reducing plasma membrane levels of calreticulin and preventing antigen presenting cell (APC) phagocytosis and T cell activation.[70] This inhibition of APC phagocytosis by STC-1 in tumors may contribute to immune evasion and resistance to immunotherapy. STC-1 might protect cone photoreceptors, at least in part, through a similar mechanism of immune evasion.

Moreover, retinal inflammation has been reported in association with photoreceptor degeneration, including upregulation of the NLRP3 inflammasome pathway, in various forms of RP.[11,71-73] In mononuclear phagocytes, treatment with *N*-acetylcysteine (NAC, inhibitor of NLRP3) downregulates inflammatory pathways by reducing NLRP3 expression and inflammatory cytokine release.[74] Interestingly,

NAC also promotes long-term survival and function of cones in rodent models of RP by reducing oxidative stress.[75] Nod-like receptor (NLR) proteins are the sensing components of inflammasome complexes, with NLRP3 being the most widely studied.[76] Recent evidence shows that NLRP3, IL-1b and c-caspase-1 are highly expressed in degenerated retinal tissue,[10] suggesting that activation of NLRP3 inflammasome plays an important role in the pathogenesis of retinal degeneration. Activated NLRP3 polymerizes and combines with apoptosis-associated speck-like protein adaptor, which then induces the activation of c-caspase-1.[77,78] Caspase-1 is responsible for triggering the activation and secretion of mature forms of inflammatory cytokines, including IL-18 and IL-1β.[77] In the current study, we found that STC-1 decreased the expression levels of NLRP3, c-caspase-1, and IL-1β in TG P23H pig retina (Figure 7). However, the origin of the inflammatory response during retinal degeneration is still controversial[79,80] and may arise from microglial activation, photoreceptor cell death, and/or other triggers. Further studies are needed to examine the association or link between microglial activation and NLRP3 signaling in RP progression in this large animal model.

Much attention regarding the current treatment approach for retinal degeneration is being focused on gene replacement therapy with viral vector–based gene delivery in order to express normal protein in the retina.[81] Gene therapy has been used for RPE65-related Leber congenital amaurosis,[82-84] which is a form of retinal degeneration causing early childhood blindness. The rate of photoreceptor degeneration after gene therapy has been observed to be the same in treated and nontreated eyes.[85-88] CRISPR (Clustered Regularly Interspaced Short Palindromic Repeats)–Cas9 gene editing is currently being investigated in animal models and human induced pluripotent stem cells to treat inherited retinal degeneration.[89,90] The duration of therapeutic effect as well as potential off-target and long-term adverse effects of genome engineering are unknown.[91-93] Additional approaches aimed at preventing further photoreceptor cell death may be needed. A therapeutic strategy that promotes cone survival and delays or halts cone cell death, allowing for preservation of central vision, would provide a major medical advance for patients with inherited and acquired forms of retinal degeneration. Based on our previous and current studies, the protective effect of STC-1 on cone photoreceptor cells was confirmed in both small and large animal models of inherited retinal degeneration with different gene mutations.[41,42] Therefore, the protective effect of STC-1 is independent of specific gene mutations. The homeostatic and pro-survival functions of STC-1 suggest that this unique polypeptide might serve as a therapeutic agent or an adjuvant to gene therapy or other therapeutic approaches.

In conclusion, our study demonstrates the protective effects of STC-1 in rescuing cone photoreceptor degeneration in the TG P23H pig, a large animal model of RP. We have found that retinal function and morphology improve after intravitreal administration of recombinant STC-1. STC-1 treatment upregulates photoreceptor specific genes and decreases expression of the NLRP3–IL-1β inflammation cascade and oxidative damage in the TG P23H pig retina, consistent with anti-inflammatory and antioxidative functions. Further mechanistic studies are required to elucidate the rescue effect(s) of STC-1 in retinal degeneration; however, the results herein provide an impetus for future preclinical studies in large animal models and eventually clinical trials in humans with retinal degeneration.

Funding/Support: Funding was provided by the Liles Macular Degeneration Research Fund (RR); Kruse Chair Endowment (LK); Baylor Scott & White-Central Texas Foundation (RR, LK); and Retina Research Foundation (LK). Financial Disclosures: All authors have no other financial relationships to disclose relevant to the contents of this paper. All authors attest that they meet the current ICMJE criteria for authorship. Contributions of Authors: Study design (RR, WX, MZ, GR); data collection (RR, WX, MZ, ST, MS); data analysis and interpretation (RR, WX, MZ, TH, LK); manuscript preparation (RR, WX, MZ); manuscript review (RR, TH, LK); administrative, technical, or logistic support (RR, WX, MZ, TH, LK, GR, LP). Other Acknowledgments: The P23H RHO transgenic pigs were obtained from the National Swine Resource and Research Center, University of Missouri, Columbia, MO (U42OD011140). The manuscript underwent subsequent peer review by the Journal and has been modified following the peer review process.

REFERENCES

1. Fahim AT, Daiger SP, Weleber RG. Nonsyndromic retinitis pigmentosa overview. In: Adam MP, Ardinger HH, Pagon RA, et al, eds. *GeneReviews*. (www.genereviews.org). Seattle, University of Washington, 1993-2021.
2. Dryja TP, McGee TL, Reichel E, et al. A point mutation of the rhodopsin gene in one form of retinitis pigmentosa. *Nature*. 1990;343(6256):364–366.
3. Paquet-Durand F, Silva J, Talukdar T, et al. Excessive activation of poly(ADP-ribose) polymerase contributes to inherited photoreceptor degeneration in the retinal degeneration 1 mouse. *J Neurosci*. 2007;27(38):10311–10319.
4. Carter-Dawson LD, LaVail MM, Sidman RL. Differential effect of the rd mutation on rods and cones in the mouse retina. *Invest Ophthalmol Vis Sci*. 1978;17(6):489–498.
5. Komeima K, Rogers BS, Lu L, Campochiaro PA. Antioxidants reduce cone cell death in a model of retinitis pigmentosa. *Proc Natl Acad Sci U S A*. 2006;103(30):11300–11305.
6. Garafalo AV, Cideciyan AV, Heon E, et al. Progress in treating inherited retinal diseases: early subretinal gene therapy clinical trials and candidates for future initiatives. *Prog Retin Eye Res*. 2020;77:100827.
7. Scholl HP, Strauss RW, Singh MS, et al. Emerging therapies for inherited retinal degeneration. *Sci Transl Med*. 2016;8(368):368rv6.

8. Roosing S, Thiadens AA, Hoyng CB, Klaver CC, den Hollander AI, Cremers FP. Causes and consequences of inherited cone disorders. *Prog Retin Eye Res*. 2014;42:1–26.
9. Narayan DS, Wood JP, Chidlow G, Casson RJ. A review of the mechanisms of cone degeneration in retinitis pigmentosa. *Acta Ophthalmol*. 2016;94(8):748–754.
10. Viringipurampeer IA, Metcalfe AL, Bashar AE, et al. NLRP3 inflammasome activation drives bystander cone photoreceptor cell death in a P23H rhodopsin model of retinal degeneration. *Hum Mol Genet*. 2016;25(8):1501–1516.
11. Noailles A, Maneu V, Campello L, Gomez-Vicente V, Lax P, Cuenca N. Persistent inflammatory state after photoreceptor loss in an animal model of retinal degeneration. *Sci Rep*. 2016;6:33356.
12. Yoshida N, Ikeda Y, Notomi S, et al. Clinical evidence of sustained chronic inflammatory reaction in retinitis pigmentosa. *Ophthalmology*. 2013;120(1):100–105.
13. Lafeber FP, Hanssen RG, Choy YM, et al. Identification of hypocalcin (teleocalcin) isolated from trout Stannius corpuscles. *Gen Comp Endocrinol*. 1988;69(1):19–30.
14. Wagner GF, Hampong M, Park CM, Copp DH. Purification, characterization, and bioassay of teleocalcin, a glycoprotein from salmon corpuscles of Stannius. *Gen Comp Endocrinol*. 1986;63(3):481–491.
15. Wagner GF, Guiraudon CC, Milliken C, Copp DH. Immunological and biological evidence for a stanniocalcin–like hormone in human kidney. *Proc Natl Acad Sci U S A*. 1995;92(6):1871–1875.
16. Ishibashi K, Imai M. Prospect of a stanniocalcin endocrine/paracrine system in mammals. *Am J Physiol Renal Physiol*. 2002;282(3):F367–F375.
17. Yeung BH, Law AY, Wong CK. Evolution and roles of stanniocalcin. *Mol Cell Endocrinol*. 2012;349(2):272–280.
18. Wagner GF, Dimattia GE. The stanniocalcin family of proteins. *J Exp Zool A Comp Exp Biol*. 2006;305(9):769–780.
19. Filvaroff EH, Guillet S, Zlot C, et al. Stanniocalcin 1 alters muscle and bone structure and function in transgenic mice. *Endocrinology*. 2002;143(9):3681–3690.
20. He LF, Wang TT, Gao QY, et al. Stanniocalcin-1 promotes tumor angiogenesis through up-regulation of VEGF in gastric cancer cells. *J Biomed Sci*. 2011;18(1):39.
21. Chakraborty A, Brooks H, Zhang P, et al. Stanniocalcin-1 regulates endothelial gene expression and modulates transendothelial migration of leukocytes. *Am J Physiol Renal Physiol*. 2007;292(2):F895–F904.
22. Zlot C, Ingle G, Hongo J, et al. Stanniocalcin 1 is an autocrine modulator of endothelial angiogenic responses to hepatocyte growth factor. *J Biol Chem*. 2003;278(48):47654–47659.
23. Law AY, Wong CK. Stanniocalcin-1 and -2 promote angiogenic sprouting in HUVECs via VEGF/VEGFR2 and angiopoietin signaling pathways. *Mol Cell Endocrinol*. 2013;374(1-2):73–81.
24. Basini G, Bussolati S, Santini SE, Grasselli F. Stanniocalcin, a potential ovarian angiogenesis regulator, does not affect endothelial cell apoptosis. *Ann N Y Acad Sci*. 2009;1171:94–99.
25. Hasilo CP, McCudden CR, Gillespie JR, et al. Nuclear targeting of stanniocalcin to mammary gland alveolar cells during pregnancy and lactation. *Am J Physiol Endocrinol Metab*. 2005;289(4):E634–E642.
26. Westberg JA, Serlachius M, Lankila P, Penkowa M, Hidalgo J, Andersson LC. Hypoxic preconditioning induces neuroprotective stanniocalcin-1 in brain via IL-6 signaling. *Stroke*. 2007;38(3):1025–1030.
27. Block GJ, Ohkouchi S, Fung F, et al. Multipotent stromal cells are activated to reduce apoptosis in part by upregulation and secretion of stanniocalcin-1. *Stem Cells*. 2009;27(3):670–681.
28. Oh JY, Ko JH, Lee HJ, et al. Mesenchymal stem/stromal cells inhibit the NLRP3 inflammasome by decreasing mitochondrial reactive oxygen species. *Stem Cells*. 2014;32(6):1553–1563.
29. Wu LM, Guo R, Hui L, et al. Stanniocalcin-1 protects bovine intestinal epithelial cells from oxidative stress-induced damage. *J Vet Sci*. 2014;15(4):475–483.
30. Mohammadipoor A, Lee RH, Prockop DJ, Bartosh TJ. Stanniocalcin-1 attenuates ischemic cardiac injury and response of differentiating monocytes/macrophages to inflammatory stimuli. *Transl Res*. 2016;177:127–142.
31. Huang L, Zhang L, Ju H, et al. Stanniocalcin-1 inhibits thrombin-induced signaling and protects from bleomycin-induced lung injury. *Sci Rep*. 2015;5:18117.
32. Liu D, Shang H, Liu Y. Stanniocalcin-1 protects a mouse model from renal ischemia-reperfusion injury by affecting ROS-mediated multiple signaling pathways. *Int J Mol Sci*. 2016;17(7):1051.
33. Durukan Tolvanen A, Westberg JA, Serlachius M, et al. Stanniocalcin 1 is important for poststroke functionality, but dispensable for ischemic tolerance. *Neuroscience*. 2013;229:49–54.
34. Kim SJ, Ko JH, Yun JH, et al. Stanniocalcin-1 protects retinal ganglion cells by inhibiting apoptosis and oxidative damage. *PLoS One*. 2013;8(5):e63749.
35. Bonfante S, Joaquim L, Fileti ME, et al. Stanniocalcin 1 inhibits the inflammatory response in microglia and protects against sepsis-associated encephalopathy. *Neurotox Res*. 2021;39(2):119–132.
36. Zhao M, Xie W, Tsai SH, et al. Intravitreal stanniocalcin-1 enhances new blood vessel growth in a rat model of laser-induced choroidal neovascularization. *Invest Ophthalmol Vis Sci*. 2018;59(2):1125–1133.
37. Dalvin LA, Hartnett ME, Bretz CA, et al. Stanniocalcin-1 is a modifier of oxygen-induced retinopathy severity. *Curr Eye Res*. 2020;45(1):46–51.
38. Roddy GW, Viker KB, Winkler NS, et al. Stanniocalcin-1 is an ocular hypotensive agent and a downstream effector molecule that is necessary for the intraocular pressure-lowering effects of latanoprost. *Invest Ophthalmol Vis Sci*. 2017;58(5):2715–2724.
39. Roddy GW, Rinkoski TA, Monson KJ, Chowdhury UR, Fautsch MP. Stanniocalcin-1 (STC-1), a downstream effector molecule in latanoprost signaling, acts independent of the FP receptor for intraocular pressure reduction. *PLoS One*. 2020;15(5):e0232591.
40. Roddy GW, Chowdhury UR, Monson KJ, Fautsch MP. Stanniocalcin-1 reduced intraocular pressure in two models of ocular hypertension. *Curr Eye Res*. 2021;46(10):1525–1530.
41. Roddy GW, Rosa Jr RH, Oh JY, et al. Stanniocalcin-1 rescued photoreceptor degeneration in two rat models of inherited retinal degeneration. *Mol Ther*. 2012;20(4):788–797.
42. Roddy GW, Yasumura D, Matthes MT, et al. Long-term photoreceptor rescue in two rodent models of retinitis pigmentosa by adeno-associated virus delivery of Stanniocalcin-1. *Exp Eye Res*. 2017;165:175–181.

43. Scott PA, de Castro JP, DeMarco PJ, et al. Progression of Pro23His retinopathy in a miniature swine model of retinitis pigmentosa. *Transl Vis Sci Technol*. 2017;6(2):4.
44. Fernandez de Castro JP, Scott PA, Fransen JW, et al. Cone photoreceptors develop normally in the absence of functional rod photoreceptors in a transgenic swine model of retinitis pigmentosa. *Invest Ophthalmol Vis Sci*. 2014;55(4):2460–2468.
45. Xie W, Zhao M, Tsai SH, et al. Correlation of spectral domain optical coherence tomography with histology and electron microscopy in the porcine retina. *Exp Eye Res*. 2018;177:181–190.
46. Xie W, Zhao M, Tsai S-H, et al. Data on SD-OCT image acquisition, ultrastructural features, and horizontal tissue shrinkage in the porcine retina. *Data Brief*. 2018;21:1019–1025.
47. Xie W, M Zhao, S Tsai, Su M, Hein TW, Kuo L, Rosa RH. Stanniocalcin-1 enhances ellipsoid zone intensity and cone function in the P23H rhodopsin transgenic pig. *Invest Ophthalmol Vis Sci*. 2019;60:452.
48. Ha A, Kim YK, Jeoung JW, Park KH. Ellipsoid zone change according to glaucoma stage advancement. *Am J Ophthalmol*. 2018;192:1–9.
49. Hood DC, Zhang X, Ramachandran R, et al. The inner segment/outer segment border seen on optical coherence tomography is less intense in patients with diminished cone function. *Invest Ophthalmol Vis Sci*. 2011;52(13):9703–9709.
50. LaVail MM, Nishikawa S, Steinberg RH, et al. Phenotypic characterization of P23H and S334ter rhodopsin transgenic rat models of inherited retinal degeneration. *Exp Eye Res*. 2018;167:56–90.
51. Garcia-Ayuso D, Ortin-Martinez A, Jimenez-Lopez M, et al. Changes in the photoreceptor mosaic of P23H-1 rats during retinal degeneration: implications for rod-cone dependent survival. *Invest Ophthalmol Vis Sci*. 2013;54(8):5888–5900.
52. Sotoca JV, Alvarado JC, Fuentes-Santamaria V, Martinez–Galan JR, Caminos E. Hearing impairment in the P23H-1 retinal degeneration rat model. *Front Neurosci*. 2014;8:297.
53. Hendrickson A, Hicks D. Distribution and density of medium- and short-wavelength selective cones in the domestic pig retina. *Exp Eye Res*. 2002;74(4):435–444.
54. Curcio CA, Sloan KR, Kalina RE, Hendrickson AE. Human photoreceptor topography. *J Comp Neurol*. 1990;292(4):497–523.
55. Bloodworth Jr JM, Gutgesell Jr HP, Engerman RL. Retinal vasculature of the pig. Light and electron microscope studies. *Exp Eye Res*. 1965;4(3):174–178.
56. Brant Fernandes RA, Koss MJ, Falabella P, et al. An innovative surgical technique for subretinal transplantation of human embryonic stem cell-derived retinal pigmented epithelium in Yucatan mini pigs: preliminary results. *Ophthalmic Surg Lasers Imaging Retina*. 2016;47(4):342–351.
57. Fouquet S, Vacca O, Sennlaub F, Paques M. The 3D retinal capillary circulation in pigs reveals a predominant serial organization. *Invest Ophthalmol Vis Sci*. 2017;58(13):5754–5763.
58. Rootman J. Vascular system of the optic nerve head and retina in the pig. *Br J Ophthalmol*. 1971;55(12):808–819.
59. Middleton S. Porcine ophthalmology. *Vet Clin North Am Food Anim Pract*. 2010;26(3):557–572.
60. Hein TW, Xu W, Xu X, Kuo L. Acute and chronic hyperglycemia elicit JIP1/JNK-mediated endothelial vasodilator dysfunction of retinal arterioles. *Invest Ophthalmol Vis Sci*. 2016;57(10):4333–4340.
61. Hein TW, Rosa Jr RH, Yuan Z, Roberts E, Kuo L. Divergent roles of nitric oxide and rho kinase in vasomotor regulation of human retinal arterioles. *Invest Ophthalmol Vis Sci*. 2010;51(3):1583–1590.
62. W Xie, M Zhao, S Tsai, M Su, TW Hein, L Kuo, RH Rosa. Progression of photoreceptor degeneration in a porcine model of retinitis pigmentosa. *Invest Ophthalmol Vis Sci*. 2017;58:274.
63. Gin TJ, Wu Z, Chew SK, Guymer RH, Luu CD. Quantitative analysis of the ellipsoid zone intensity in phenotypic variations of intermediate age-related macular degeneration. *Invest Ophthalmol Vis Sci*. 2017;58(4):2079–2086.
64. Routledge D, Scholpp S. Mechanisms of intercellular Wnt transport. *Development*. 2019;146(10):dev176073.
65. Ruan Y, Ogana H, Gang E, Kim HN, Kim YM. Wnt signaling in the tumor microenvironment. *Adv Exp Med Biol*. 2021;1270:107–121.
66. Yoshiko Y, Aubin JE. Stanniocalcin 1 as a pleiotropic factor in mammals. *Peptides*. 2004;25(10):1663–1669.
67. Usui S, Oveson BC, Lee SY, et al. NADPH oxidase plays a central role in cone cell death in retinitis pigmentosa. *J Neurochem*. 2009;110(3):1028–1037.
68. Wang Y, Huang L, Abdelrahim M, et al. Stanniocalcin-1 suppresses superoxide generation in macrophages through induction of mitochondrial UCP2. *J Leukoc Biol*. 2009;86(4):981–988.
69. McCudden CR, James KA, Hasilo C, Wagner GF. Characterization of mammalian stanniocalcin receptors. Mitochondrial targeting of ligand and receptor for regulation of cellular metabolism. *J Biol Chem*. 2002;277(47):45249–45258.
70. Lin H, Kryczek I, Li S, et al. Stanniocalcin 1 is a phagocytosis checkpoint driving tumor immune resistance. *Cancer Cell*. 2021;39(4):480–493.
71. Rana T, Shinde VM, Starr CR, et al. An activated unfolded protein response promotes retinal degeneration and triggers an inflammatory response in the mouse retina. *Cell Death Dis*. 2014;5:e1578.
72. Appelbaum T, Santana E, Aguirre GD. Strong upregulation of inflammatory genes accompanies photoreceptor demise in canine models of retinal degeneration. *PLoS One*. 2017;12(5):e0177224.
73. Sudharsan R, Beiting DP, Aguirre GD, Beltran WA. Involvement of innate immune system in late stages of inherited photoreceptor degeneration. *Sci Rep*. 2017;7(1):17897.
74. Liu Y, Yao W, Xu J, et al. The anti-inflammatory effects of acetaminophen and N-acetylcysteine through suppression of the NLRP3 inflammasome pathway in LPS-challenged piglet mononuclear phagocytes. *Innate Immun*. 2015;21(6):587–597.
75. Lee SY, Usui S, Zafar AB, et al. N-acetylcysteine promotes long-term survival of cones in a model of retinitis pigmentosa. *J Cell Physiol*. 2011;226(7):1843–1849.
76. Haneklaus M, O'Neill LA. NLRP3 at the interface of metabolism and inflammation. *Immunol Rev*. 2015;265(1):53–62.
77. Wooff Y, Fernando N, Wong JHC, et al. Caspase-1-dependent inflammasomes mediate photoreceptor cell death in photo-oxidative damage-induced retinal degeneration. *Sci Rep*. 2020;10(1):2263.

78. He Y, Hara H, Nunez G. Mechanism and regulation of NLRP3 inflammasome activation. *Trends Biochem Sci*. 2016;41(12):1012–1021.
79. Campochiaro PA, Mir TA. The mechanism of cone cell death in retinitis pigmentosa. *Prog Retin Eye Res*. 2018;62:24–37.
80. Rashid K, Akhtar-Schaefer I, Langmann T. Microglia in retinal degeneration. *Front Immunol*. 2019;10:1975.
81. Arbabi A, Liu A, Ameri H. Gene therapy for inherited retinal degeneration. *J Ocul Pharmacol Ther*. 2019;35(2):79–97.
82. Bainbridge JW, Smith AJ, Barker SS, et al. Effect of gene therapy on visual function in Leber's congenital amaurosis. *N Engl J Med*. 2008;358(21):2231–2239.
83. Maguire AM, Simonelli F, Pierce EA, et al. Safety and efficacy of gene transfer for Leber's congenital amaurosis. *N Engl J Med*. 2008;358(21):2240–2248.
84. Hauswirth WW, Aleman TS, Kaushal S, et al. Treatment of Leber congenital amaurosis due to RPE65 mutations by ocular subretinal injection of adeno-associated virus gene vector: short-term results of a phase I trial. *Hum Gene Ther*. 2008;19(10):979–990.
85. Jacobson SG, Cideciyan AV, Roman AJ, et al. Improvement and decline in vision with gene therapy in childhood blindness. *N Engl J Med*. 2015;372(20):1920–1926.
86. Bainbridge JW, Mehat MS, Sundaram V, et al. Long-term effect of gene therapy on Leber's congenital amaurosis. *N Engl J Med*. 2015;372(20):1887–1897.
87. Maguire AM, Russell S, Wellman JA, et al. Efficacy, safety, and durability of voretigene neparvovec-rzyl in RPE65 mutation-associated inherited retinal dystrophy: results of phase 1 and 3 trials. *Ophthalmology*. 2019;126(9):1273–1285.
88. Sengillo JD, Gregori NZ, Sisk RA, et al. Visual acuity, retinal morphology, and patients' perceptions after voretigene neparvovec-rzyl for RPE65-associated retinal disease. *Ophthalmol Retina*. 2021 S2468-6350(21)00378-X. doi:10.1016/j.oret.2021.11.005.
89. Sanjurjo-Soriano C, Erkilic N, Baux D, et al. Genome editing in patient iPSCs corrects the most prevalent USH2A mutations and reveals intriguing mutant mRNA expression profiles. *Mol Ther Methods Clin Dev*. 2020;17:156–173.
90. Burnight ER, Giacalone JC, Cooke JA, et al. CRISPR-Cas9 genome engineering: Treating inherited retinal degeneration. *Prog Retin Eye Res*. 2018;65:28–49.
91. Bucher K, Rodríguez-Bocanegra E, Dauletbekov D, Fischer MD. Immune responses to retinal gene therapy using adeno-associated viral vectors–implications for treatment success and safety. *Prog Retin Eye Res*. 2021;83:100915.
92. Quinn J, Musa A, Kantor A, et al. Genome-editing strategies for treating human retinal degenerations. *Hum Gene Ther*. 2021;32(5-6):247–259.
93. Yu W, Wu Z. Ocular delivery of CRISPR/Cas genome editing components for treatment of eye diseases. *Adv Drug Deliv Rev*. 2021;168:181–195.